Second harmonic generation from tetragonal centrosymmetric crystals

Shengyuan A. Yang and Xiaoqin Li
Department of Physics, Texas Materials Institute, The University of Texas, Austin, Texas 78712, USA

Alan D. Bristow and J. E. Sipe*
JILA, National Institute of Standards and Technology, University of Colorado, Boulder, Colorado 80309-0440, USA
(Received 26 May 2009; revised manuscript received 8 September 2009; published 5 October 2009)

We present a phenomenological theory of second harmonic generation (SHG) from tetragonal centrosymmetric crystals. It includes the lowest order bulk response, which is of electric quadrupole and magnetic dipole symmetry, and the lowest order surface response, which is of electric dipole symmetry. Based on the symmetry properties of the nonlinear response tensor, complete expressions are obtained for the SHG expected in reflection from a crystal with a (001) surface orientation. We suggest experimental configurations that can be used to extract particular tensor elements. We find that dichroism is present in SHG from tetragonal centrosymmetric crystals, although the crystal is not chiral.

DOI: 10.1103/PhysRevB.80.165306 PACS number(s): 42.65.Ky, 78.20.Bh

I. INTRODUCTION

Optical second harmonic generation (SHG) has been widely used as a noninvasive and noncontact probe of the electronic and structural properties of crystals.[1] For crystals without inversion symmetry, the dominant contribution to SHG comes from the bulk electric dipole response. For media with inversion symmetry, such an electric dipole response is forbidden in bulk, but is allowed within a few atomic layers of surfaces and interfaces. It has been demonstrated experimentally that the SHG from these surface contributions is usually comparable to, or even stronger than, the contributions arising from higher-order sources in the bulk with electric quadrupole and magnetic dipole symmetry.[2–4] As a result, SHG has proven to be a powerful tool for investigating surfaces of centrosymmetric crystals, and more generally interfaces between centrosymmetric media, even when they are buried inside a multilayer structure.[5] Typically, careful analysis of experimental data is required to extract information about surfaces and interfaces.

A phenomenological approach to describing SHG from cubic and isotropic media was developed in the 1960s,[6–8] and later extended to include anisotropic effects by Sipe *et al.*[9] The general strategy is to analyze the results of SHG measurements purely from the macroscopic symmetry of the medium, taking into account both bulk and surface effects, with no assumption of the microscopic origin of the macroscopic response tensors. Such a phenomenological approach has been successfully applied to explain experimental results and to provide guidance in designing experiments. It also serves as a preliminary step to further theoretical studies based on microscopic approaches. The most extensive use of the phenomenological models is limited to cubic- or diamond-based lattices, because of their relatively straight forward symmetry and the commercial importance of materials such as silicon and its oxides.[10–15] Certain extensions of the SHG theory have been developed previously to treat systems with lower symmetry such as vicinal faces of cubic crystals.[16,17]

In this paper, we extend this phenomenological approach to tetragonal centrosymmetric crystals. The importance of this extension lies in the fact that many crystals in this class are of great physical interest and practical value. Piezoelectric materials such as $PbBi_2Nb_2O_9$, paraelectric materials such as $SrTiO_3$, and parent compounds of high-T_c superconductors such as $HgBa_2CuO_{4+\delta}$ (Ref. 18) all have a phase of tetragonal centrosymmetric symmetry. Therefore, the theoretical description of SHG should facilitate experimental investigations of their properties. For example, the nature of the pseudogap states in high-T_c superconductors remains an unsolved critical issue in high-T_c superconductors.[19] While many models involve additional charge orders, the vast majority of experimental studies have not shown any change in symmetry upon moving from the normal state to the pseudogap state. More recently, it has been proposed that circulating current may spontaneously form and break the time-reversal-symmetry and/or inversion symmetry.[20,21] Various experimental techniques have been proposed and implemented in search of such circulating currents. Conflicting results, however, have been reported.[22,23] Similar to broken spatial symmetry, broken time-reversal symmetry can lead to new contributions to SHG. This sensitivity to symmetry motivated proposals using SHG as a tool to study phase transitions in the cuprates.[24]

Two major complications arise in the extension of the phenomenological description to tetragonal centrosymmetric crystals. First, different polarizations of the fundamental field in the medium have different wave vectors, because of the anisotropy of the linear optical response. Second, the nonlinear susceptibility tensor in tetragonal crystals has many more nonzero components than that in cubic crystals, because of the reduced symmetry of tetragonal crystals.

This paper is organized as the following: First, in Sec. II, we describe the problem under consideration and express the fundamental fields inside the medium in terms of the incident fields. Next, in Sec. III, we calculate the bulk nonlinear polarization and obtain the corresponding SHG using a formalism based on Green functions. After that, in Sec. IV, we calculate the SHG from surface dipole contribution. In Sec. V, we discuss how our calculations can be used to guide experimental investigations, and in Sec. VI, we draw some final conclusions.

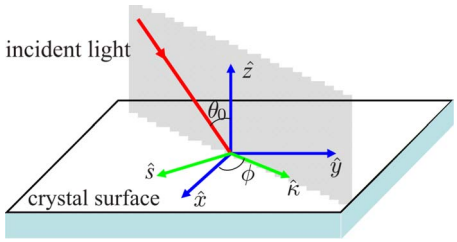

FIG. 1. (Color online) Experimental geometry with definitions of the crystal coordinate system as well as the beam coordinate system.

II. MODEL OF THE SYSTEM

In a phenomenological approach, the SHG is typically calculated in three steps: (i) Given the incident fields, the fundamental fields inside the nonlinear medium are calculated solely on the basis of the linear response of the medium. Since SHG and other nonlinear effects are weak, and pump depletion can be neglected, this approach provides a good approximation of the actual fundamental fields in the medium. (ii) The second harmonic polarization of the medium (both bulk and surface contributions) is written in terms of the fundamental fields and the second-order susceptibility tensors. (iii) The second harmonic fields outside the medium that are generated by the nonlinear polarization are calculated.

In this section, we address the first of these three steps. Consider a tetragonal centrosymmetric crystal medium filling out the half space $z<0$ with its surface normal along the $\hat{\mathbf{z}}$ direction. We choose the three axes $(\hat{\mathbf{x}},\hat{\mathbf{y}},\hat{\mathbf{z}})$ of our lab reference frame to be along the three principal crystal axes. This coordinate system is referred to as the crystal coordinate system.

A laser beam, idealized as a monochromatic plane wave with a frequency ω and a wave vector $\boldsymbol{\nu}_{0-}$, is incident on the medium at an angle θ_0 (cf. Fig. 1). The incident field can be expressed as

$$\mathbf{E}_0(\mathbf{r},t) = \mathbf{E}_0 e^{i\boldsymbol{\nu}_{0-}\cdot\mathbf{r}-i\omega t} + c\,.\,c\,. \tag{1}$$

The beam coordinate system is defined as $(\hat{\mathbf{s}},\hat{\boldsymbol{\kappa}},\hat{\mathbf{z}})$, by taking $\hat{\boldsymbol{\kappa}}$ to be the direction identified by the projection of $\boldsymbol{\nu}_{0-}$ on the (xy) plane, and $\hat{\mathbf{s}}=\hat{\boldsymbol{\kappa}}\times\hat{\mathbf{z}}$, as sketched in Fig. 1.

The bases of crystal and beam coordinate systems are related to each other by an orthogonal transformation,

$$\begin{pmatrix}\hat{\mathbf{s}}\\ \hat{\boldsymbol{\kappa}}\\ \hat{\mathbf{z}}\end{pmatrix} = V\begin{pmatrix}\hat{\mathbf{x}}\\ \hat{\mathbf{y}}\\ \hat{\mathbf{z}}\end{pmatrix}, \tag{2}$$

where

$$V = \begin{pmatrix}\sin\phi & -\cos\phi & 0\\ \cos\phi & \sin\phi & 0\\ 0 & 0 & 1\end{pmatrix}. \tag{3}$$

ϕ is the angle between $\hat{\mathbf{x}}$ and $\hat{\boldsymbol{\kappa}}$, as shown in Fig. 1. The incident wave vector has a component $\boldsymbol{\kappa}=\hat{\boldsymbol{\kappa}}|\boldsymbol{\nu}_{0-}|\sin\theta_0$ in the (xy) plane. Given the magnitude of the wave vector $|\boldsymbol{\nu}_{0-}| = \omega/c \equiv \tilde{\omega}$, the wave vector can be written as

$$\boldsymbol{\nu}_{0-} = \boldsymbol{\kappa} - w_0\hat{\mathbf{z}}, \tag{4}$$

with

$$w_0 = (\tilde{\omega}^2 - \kappa^2)^{1/2}. \tag{5}$$

Throughout this paper, the square root function of a (in general) complex number z, $\sqrt{z}$, is defined such that $\mathrm{Im}\,\sqrt{z}\geq 0$ and, if $\mathrm{Im}\,\sqrt{z}=0$, $\mathrm{Re}\,\sqrt{z}\geq 0$. The decomposition of the field into s- and p-polarization is written as

$$\mathbf{E}_0 = E_{0p}\hat{\mathbf{p}}_{0-} + E_{0s}\hat{\mathbf{s}} \tag{6}$$

where the unit vector for p-polarization is

$$\hat{\mathbf{p}}_{0-} = \frac{\kappa\hat{\mathbf{z}} + w_0\hat{\boldsymbol{\kappa}}}{\tilde{\omega}}. \tag{7}$$

We now write down the general form of the fundamental fields inside the medium. For tetragonal crystals with (001) crystal surface orientation, the linear optical property of the medium can be characterized by the following dielectric tensor,

$$\boldsymbol{\epsilon}(\omega) = \begin{bmatrix}\epsilon^{\parallel} & 0 & 0\\ 0 & \epsilon^{\parallel} & 0\\ 0 & 0 & \epsilon^{\perp}\end{bmatrix}, \tag{8}$$

where both $\epsilon^{\parallel}$ and $\epsilon^{\perp}$ can be complex numbers. As required by the Maxwell equations, the field inside the medium takes the general form[25]

$$\mathbf{E}(\mathbf{r},t) = \mathbf{E}(\mathbf{r})e^{-i\omega t} + c\,.\,c\,., \tag{9}$$

where

$$\mathbf{E}(\mathbf{r}) = \hat{\mathbf{s}}E_s e^{i\boldsymbol{\nu}_-^s\cdot\mathbf{r}} + \mathbf{q}_- E_p e^{i\boldsymbol{\nu}_-^p\cdot\mathbf{r}}. \tag{10}$$

The s- and p-polarization components acquire different wave vectors

$$\boldsymbol{\nu}_-^s = \boldsymbol{\kappa} - w^s\hat{\mathbf{z}}, \quad w^s = \sqrt{\tilde{\omega}^2\epsilon^{\parallel} - \kappa^2}, \tag{11a}$$

$$\boldsymbol{\nu}_-^p = \boldsymbol{\kappa} - w^p\hat{\mathbf{z}}, \quad w^p = \sqrt{\tilde{\omega}^2\epsilon^{\parallel} - \frac{\epsilon^{\parallel}}{\epsilon^{\perp}}\kappa^2}. \tag{11b}$$

The p-polarization direction is specified by

$$\mathbf{q}_- \equiv \frac{n}{\tilde{\omega}}\left[\frac{\kappa}{\epsilon^{\perp}}\hat{\mathbf{z}} + \frac{w^p}{\epsilon^{\parallel}}\hat{\boldsymbol{\kappa}}\right], \tag{12}$$

where $n \equiv \sqrt{\boldsymbol{\nu}_-^s\cdot\boldsymbol{\nu}_-^s}/\tilde{\omega} = \sqrt{\epsilon^{\parallel}}$ is the index of refraction for the s-polarized wave. Note that the polarization vector $\mathbf{q}_-$ is not a unit vector. To simplify the notation below, we write

$$\mathbf{q}_- = f_s\hat{\mathbf{z}} + f_c\hat{\boldsymbol{\kappa}}, \tag{13}$$

where the factors f_s and f_c are obtained from Eq. (12). For cubic crystals, if n is real, then f_s and f_c will correspond to the sine and cosine of the angle of the beam propagation inside the crystal. For tetragonal crystals, however, f_s and f_c depend on this angle in a more complicated way.

Despite the anisotropy [Eq. (8)] of the dielectric tensor, *s*- and *p*-polarized components of an incident beam do not mix at an interface. Therefore, reflection and transmission calculations can still be performed for one polarization at a time, as in the case with isotropic media. However, the Fresnel coefficients take a different form. For light incident from medium i to medium j, if the vectors $\hat{\mathbf{s}}$ and $\mathbf{q}_-$ are used to reference the amplitudes, the transmission Fresnel coefficients are[25]

$$t_{ij}^s = \frac{2w_i^s}{w_i^s + w_j^s}, \quad t_{ij}^p = \frac{2n_i n_j w_i^p}{w_i^p \epsilon_j^{\parallel} + w_j^p \epsilon_i^{\parallel}}, \tag{14}$$

for *s*- and *p*-polarizations, respectively.

For a half space calculation, $i=0$ and $j=1$ refer to the vacuum (or air) and the crystal, respectively. Thus, we have $w_0^s = w_0^p = w_0$, and $n_0 = \sqrt{\epsilon_0^{\parallel}} = 1$. The fundamental field in the nonlinear medium is given by Eq. (10), with

$$E_s = t_{01}^s E_{0s}, \quad t_{01}^s = \frac{2w_0}{w_0 + w^s}, \tag{15a}$$

$$E_p = t_{01}^p E_{0p}, \quad t_{01}^p = \frac{2nw_0}{w_0 \epsilon^{\parallel} + w^p}. \tag{15b}$$

Once the fundamental fields inside the medium are known, we can calculate the nonlinear polarizations.

III. BULK CONTRIBUTION

In this section, we calculate the SHG in reflection from the bulk crystal. To do so, we first determine the nonlinear polarization from the fundamental fields inside the medium. The SHG is then calculated using a Green's function formalism.

For a crystal with inversion symmetry, such as a tetragonal centrosymmetric crystal, the second order dipole response tensor $\chi^{(2)}$ from bulk crystal vanishes identically. The lowest order nonlinear response comes from higher order nonlocal sources with either electric quadrupole or magnetic dipole symmetry.[7] This response can, in general, be expressed in terms of an effective polarization

$$P_i^b(\mathbf{r},t) = P_i^{b(2\omega)}(\mathbf{r}) e^{-2i\omega t} + c.c., \tag{16}$$

where

$$P_i^{b(2\omega)}(\mathbf{r}) = \Gamma_{ijkl} E_j(\mathbf{r}) \frac{\partial}{\partial x_k} E_l(\mathbf{r}), \tag{17}$$

and where the superscript b indicates a bulk contribution and summation over repeated indices is assumed. Although the exact value of the fourth rank response tensor Γ_{ijkl} should be determined from microscopic theory, its form is dictated by the symmetry property of the crystal. Tetragonal crystals with inversion symmetry fall into two classes of point group symmetry: C_{4h} and D_{4h} ($4/m$ and $4/mmm$ in the international notation). For both classes of crystals, when written in the crystal coordinate system, there are 21 nonzero elements of Γ_{ijkl}, of which only 11 are independent;[26] these are $\Gamma_{xxxx} = \Gamma_{yyyy}$, Γ_{zzzz}, $\Gamma_{yyzz} = \Gamma_{xxzz}$, $\Gamma_{yzzy} = \Gamma_{xzzx}$, $\Gamma_{xxyy} = \Gamma_{yyxx}$, $\Gamma_{zzyy} = \Gamma_{zzxx}$, $\Gamma_{yzyz} = \Gamma_{xzxz}$, $\Gamma_{xyxy} = \Gamma_{yxyx}$, $\Gamma_{zyyz} = \Gamma_{zxxz}$, $\Gamma_{zyzy} = \Gamma_{zxzx}$, and $\Gamma_{xyyx} = \Gamma_{yxxy}$. However, the simplest type of SHG experiment, which relies on only one fundamental incident beam, is not sensitive to all 11 independent components. To see this, we note that

$$P_i^{b(2\omega)}(\mathbf{r}) \tag{18a}$$

$$= \Gamma_{ijxl} E_j(\mathbf{r}) \frac{\partial}{\partial x} E_l(\mathbf{r}) + \Gamma_{ijyl} E_j(\mathbf{r}) \frac{\partial}{\partial y} E_l(\mathbf{r}) + \Gamma_{ijzl} E_j(\mathbf{r}) \frac{\partial}{\partial z} E_l(\mathbf{r}) \tag{18b}$$

$$= i\kappa_x \Gamma_{ijxl} E_j(\mathbf{r}) E_l(\mathbf{r}) + i\kappa_y \Gamma_{ijyl} E_j(\mathbf{r}) E_l(\mathbf{r}) + \Gamma_{ijzl} E_j(\mathbf{r}) \frac{\partial}{\partial z} E_l(\mathbf{r}) \tag{18c}$$

$$= \frac{1}{2} i\kappa_x (\Gamma_{ijxl} + \Gamma_{ilxj}) E_j(\mathbf{r}) E_l(\mathbf{r}) + \frac{1}{2} i\kappa_y (\Gamma_{ijyl} + \Gamma_{ilyj}) E_j(\mathbf{r}) E_l(\mathbf{r}) + \Gamma_{ijzl} E_j(\mathbf{r}) \frac{\partial}{\partial z} E_l(\mathbf{r}) \tag{18d}$$

$$= i\kappa_x \Gamma_{ijxl}^s E_j(\mathbf{r}) E_l(\mathbf{r}) + i\kappa_y \Gamma_{ijyl}^s E_j(\mathbf{r}) E_l(\mathbf{r}) + \Gamma_{ijzl} E_j(\mathbf{r}) \frac{\partial}{\partial z} E_l(\mathbf{r}) \tag{18e}$$

$$= \Gamma_{ijxl}^s E_j(\mathbf{r}) \frac{\partial}{\partial x} E_l(\mathbf{r}) + \Gamma_{ijyl}^s E_j(\mathbf{r}) \frac{\partial}{\partial y} E_l(\mathbf{r}) + \Gamma_{ijzl} E_j(\mathbf{r}) \frac{\partial}{\partial z} E_l(\mathbf{r}), \tag{18f}$$

where in the third and last line we have used the form (10,11) of the fundamental field $\mathbf{E}(\mathbf{r})$, in the fourth line we have used the fact that $E_j(\mathbf{r})$ and $E_l(\mathbf{r})$ refer to the same fundamental field to sum over two equivalent versions of dummy indices, and in the last two lines we have defined

$$\Gamma_{ijxl}^s \equiv \frac{1}{2}(\Gamma_{ijxl} + \Gamma_{ilxj}), \tag{19}$$

$$\Gamma_{ijyl}^s \equiv \frac{1}{2}(\Gamma_{ijyl} + \Gamma_{ilyj}). \tag{20}$$

Thus in a "single beam" experiment using only one incident fundamental beam, the SHG generated depends only on the 9 independent components that are labeled by $a_i (i = 1, \cdots, 9)$ in Table I. If both the fundamental and second harmonic frequencies are far away from any resonance in the material, one can treat the medium as dispersionless. Additional permutation symmetries lead to $\Gamma_{ijkl} = \Gamma_{jikl}$.[6] As a result, one has $a_2 = a_3$, $a_5 = a_7$, and $a_6 = a_8$.

To obtain the polarization through Eq. (17), it is convenient to perform the calculation in the beam coordinates instead of the crystal coordinates. The tensor transformation of Γ_{ijkl} from the crystal coordinates to the beam coordinates can be written as:

TABLE I. Nonzero tensor elements of Γ_{ijkl}.

$a_1=\Gamma_{xxxx}=\Gamma_{yyyy}$
$a_2=\Gamma^s_{xxyy}=\Gamma^s_{xyyx}=\Gamma^s_{yyxx}=\Gamma^s_{yxxy}$
$a_3=\Gamma_{xyxy}=\Gamma_{yxyx}$
$a_4=\Gamma_{xxzz}=\Gamma_{yyzz}$
$a_5=\Gamma_{xzzx}=\Gamma_{yzzy}$
$a_6=\Gamma_{yzyz}=\Gamma_{xzxz}$
$a_7=\Gamma_{zyzy}=\Gamma_{zxzx}$
$a_8=\Gamma^s_{zzyy}=\Gamma^s_{zyyz}=\Gamma^s_{zzxx}=\Gamma^s_{zxxz}$
$a_9=\Gamma_{zzzz}$

$$\Gamma'_{ijkl}=\sum_{i'j'k'l'} V_{ii'}V_{jj'}V_{kk'}V_{ll'}\Gamma_{i'j'k'l'}, \tag{21}$$

where the components of Γ' range over $(1,2,3)=(s,\kappa,z)$, and the components of Γ range over $(1,2,3)=(x,y,z)$; the transformation matrix V is written explicitly in Eq. (3). The components of the fundamental electric field inside the medium, expressed in the beam coordinate, are

$$E'_s=E_s e^{i\boldsymbol{\nu}^s_-\cdot\mathbf{r}}e^{-i\omega t},\quad E'_\kappa=f_c E_p e^{i\boldsymbol{\nu}^p_-\cdot\mathbf{r}}e^{-i\omega t},$$

$$E'_z=f_s E_p e^{i\boldsymbol{\nu}^p_-\cdot\mathbf{r}}e^{-i\omega t}. \tag{22}$$

Since in the crystal and beam coordinate systems we have, respectively,

$$\mathbf{r}=x\hat{\mathbf{x}}+y\hat{\mathbf{y}}+z\hat{\mathbf{z}}\equiv r_s\hat{\mathbf{s}}+r_\kappa\hat{\boldsymbol{\kappa}}+r_z\hat{\mathbf{z}}, \tag{23}$$

we can write $\exp(i\boldsymbol{\kappa}\cdot\mathbf{R})=\exp(i\kappa r_\kappa)$, where $\mathbf{R}=(x,y)$ is a shorthand notation for the coordinates in the horizontal plane. For calculations on the fundamental field Eq. (22) we have

$$\frac{\partial}{\partial r_s}\to 0,\quad \frac{\partial}{\partial r_\kappa}\to i\kappa, \tag{24}$$

and

$$\frac{\partial}{\partial r_z}=\frac{\partial}{\partial z}\to -iw^s\quad (\text{for } E'_s),$$

$$\frac{\partial}{\partial r_z}=\frac{\partial}{\partial z}\to -iw^p\quad (\text{for } E'_\kappa, E'_z). \tag{25}$$

After performing the tensor transformation and taking the derivative explicitly using Eqs. (21)–(25), we can rewrite the polarization [Eq. (17)] by defining an effective second order susceptibility M_{iln},

$$P_i^{b(2\omega)}=iM_{iln}E'_l E'_n. \tag{26}$$

This effective second order susceptibility M_{iln} is calculated and listed in Table II with (1,2,3) denoting (s,κ,z), respectively. Elements not shown in Table II are zero.

TABLE II. Nonzero tensor elements of the effective second order susceptibility tensor M_{iln} for bulk polarization.

$M_{111}=-M_{122}=-M_{221}=-M_{212}=\frac{\kappa}{4}(-a_1+2a_2+a_3)\sin 4\phi$
$M_{121}=M_{112}=\frac{\kappa}{4}[(a_1+2a_2-a_3)+(-a_1+2a_2+a_3)\cos 4\phi]$
$M_{131}=-w^s a_5$
$M_{113}=M_{223}=-w^p a_4$
$M_{211}=\frac{\kappa}{4}[(a_1-2a_2+3a_3)+(-a_1+2a_2+a_3)\cos 4\phi]$
$M_{222}=\frac{\kappa}{4}[(3a_1+2a_2+a_3)-(-a_1+2a_2+a_3)\cos 4\phi]$
$M_{232}=-w^p a_5$
$M_{233}=\kappa a_6$
$M_{311}=-w^s a_7$
$M_{322}=-w^p a_7$
$M_{332}=M_{323}=\kappa a_8$
$M_{333}=-w^p a_9$

The various physical quantities defined in Sec. II will, in general, take values at second harmonic frequency that are different from those at the fundamental. We introduce the following upper case symbols for the physical quantities at frequency 2ω.

$$\tilde{\Omega}=\frac{2\omega}{c},\quad \mathbf{K}=2\boldsymbol{\kappa}. \tag{27}$$

The wave vector components for the second harmonic field in air are

$$\mathbf{V}_{0+}=\mathbf{K}+W_0\hat{\mathbf{z}},\quad W_0=(\tilde{\Omega}^2-K^2)^{1/2}=2w_0,$$

$$\hat{\mathbf{P}}_{0\pm}=\frac{K\hat{\mathbf{z}}\mp W_0\hat{\boldsymbol{\kappa}}}{\tilde{\Omega}}. \tag{28}$$

The corresponding wave vector components for second harmonic field in the nonlinear medium are given by

$$W^s=\sqrt{\tilde{\Omega}^2\epsilon^{\parallel}(2\omega)-K^2},$$

$$W^p=\sqrt{\tilde{\Omega}^2\epsilon^{\parallel}(2\omega)-\frac{\epsilon^{\parallel}(2\omega)}{\epsilon^{\perp}(2\omega)}K^2}$$

$$\mathbf{Q}_+=\frac{N}{\tilde{\Omega}}\left[\frac{K}{\epsilon^{\perp}(2\omega)}\hat{\mathbf{z}}-\frac{W^p}{\epsilon^{\parallel}(2\omega)}\hat{\boldsymbol{\kappa}}\right]=F_s\hat{\mathbf{z}}-F_c\hat{\boldsymbol{\kappa}},$$

$$\mathbf{Q}_-=F_s\hat{\mathbf{z}}+F_c\hat{\boldsymbol{\kappa}}, \tag{29}$$

$$N\equiv\frac{V^s}{\tilde{\Omega}}=\sqrt{\epsilon^{\parallel}(2\omega)},$$

$$F_s=\frac{N}{\tilde{\Omega}}\frac{K}{\epsilon^{\perp}(2\omega)},\quad F_c=\frac{N}{\tilde{\Omega}}\frac{W^p}{\epsilon^{\parallel}(2\omega)}. \tag{30}$$

We now write down the general forms of the polarization and fields at the SHG frequency. The polarization takes the form

$$\mathbf{P}^{b(2\omega)}(\mathbf{r},t) = \mathbf{P}^{b(2\omega)}(z)e^{2i\boldsymbol{\kappa}\cdot\mathbf{R}-2i\omega t} + c\,.\,c\,. \tag{31}$$

Similarly, the electric field (both inside and outside the crystal) can be written in the form:

$$\mathbf{E}^{(2\omega)}(\mathbf{r},t) = \mathbf{E}^{(2\omega)}(z)e^{2i\boldsymbol{\kappa}\cdot\mathbf{R}-2i\omega t} + c\,.\,c\,. \tag{32}$$

Using a Green function method developed by Sipe *et al.*,[25,27] the second harmonic field both inside and outside the crystal can be determined. Suppose first that we had a crystal filling all of space, but with a polarization source confined to $z<0$. Then the generated second harmonic field would take the form

$$\mathbf{E}^{(2\omega)}(z) = \int_{-\infty}^{0} \mathcal{G}_E(z-z')\cdot\mathbf{P}^{b(2\omega)}(z')dz', \tag{33}$$

where the Green function for tetragonal centrosymmetric crystals is given by

$$\begin{aligned}\mathcal{G}_E(z-z') = {}& \frac{i\tilde{\Omega}^2}{2\varepsilon_0}\theta(z-z')\left(e^{iW^s(z-z')}\frac{\hat{\mathbf{s}}\hat{\mathbf{s}}}{W^s} + e^{iW^p(z-z')}\frac{\mathbf{Q}_+\mathbf{Q}_+}{W^p}\right)\\ &+ \frac{i\tilde{\Omega}^2}{2\varepsilon_0}\theta(z'-z)\left(e^{-iW^s(z-z')}\frac{\hat{\mathbf{s}}\hat{\mathbf{s}}}{W^s} + e^{-iW^p(z-z')}\frac{\mathbf{Q}_-\mathbf{Q}_-}{W^p}\right)\\ &- \frac{1}{\varepsilon_0\boldsymbol{\epsilon}^{\perp}(2\omega)}\delta(z-z')\hat{\mathbf{z}}\hat{\mathbf{z}},\end{aligned} \tag{34}$$

where $\theta(z)$ is the Heaviside step function. The dyadic expressions, such as $\hat{\mathbf{s}}\hat{\mathbf{s}}$, indicate $\mathcal{G}_E$ is a second rank tensor. The first term in $\mathcal{G}_E$ represents an upward propagating wave, the second term is a downward going wave, and the third term is a localized field with only a $\hat{\mathbf{z}}$ component. For the actual crystal configuration considered in this paper, where the crystal does not fill all space but extends only from $z=0$ to $z=-\infty$, it is easy[25,27] to work out the corrections to Eq. (33) as the following. Each upward-going wave contributing to Eq. (33) is incident on the interface at $z=0$, and leads to an additional wave reflected into the crystal (for $z<0$) and to a wave transmitted into vacuum (for $z>0$). The latter, which is of interest here, can be related simply to the upward-going wave in the crystal via the Fresnel coefficients at 2ω; it can clearly be separated into two polarization components,

$$\mathbf{E}^{(2\omega)}(z) = (E_s^{(2\omega)}\hat{\mathbf{s}} + E_p^{(2\omega)}\hat{\mathbf{P}}_{0+})e^{iW_0 z}, \tag{35}$$

where

$$E_s^{(2\omega)} = \frac{i\tilde{\Omega}^2 T_{10}^s}{2\varepsilon_0 W^s}\int_{-\infty}^{0} e^{-iW^s z'}\hat{\mathbf{s}}\cdot\mathbf{P}^{(2\omega)}(z')dz', \tag{36}$$

and

$$E_p^{(2\omega)} = \frac{i\tilde{\Omega}^2 T_{10}^p}{2\varepsilon_0 W^p}\int_{-\infty}^{0} e^{-iW^p z'}\mathbf{Q}_+\cdot\mathbf{P}^{(2\omega)}(z')dz', \tag{37}$$

with the two Fresnel transmission coefficients T_{10}^s and T_{10}^p,

$$T_{10}^s = \frac{2W^s}{W^s+W_0}, \quad T_{10}^p = \frac{2NW^p}{W^p+W_0\boldsymbol{\epsilon}^{\parallel}(2\omega)}. \tag{38}$$

TABLE III. The coefficients defined in Eqs. (39) and (40) for SHG from bulk nonlinear polarizations.

$A_s = -\frac{i\tilde{\Omega}^2}{\varepsilon_0(W^s+W_0)}$

$A_p = -\frac{i\tilde{\Omega}^2 N}{\varepsilon_0[W^p+W_0\epsilon^{\parallel}(2\omega)]}$

$B_{ss}^s = \frac{M_{111}}{W^s+2w^s}$

$B_{pp}^s = -\frac{M_{111}}{W^s+2w^p}f_c^2$

$B_{sp}^s = \frac{2M_{121}f_c+(M_{131}+M_{113})f_s}{W^s+w^s+w^p}$

$B_{ss}^p = \frac{F_sM_{311}-F_cM_{211}}{W^p+2w^s}$

$B_{pp}^p = \frac{1}{W^p+2w^p}[F_sM_{322}f_c^2+2F_sM_{332}f_sf_c+F_sM_{333}f_s^2 -F_cM_{222}f_c^2-F_c(M_{113}+M_{232})f_sf_c-F_cM_{233}f_s^2]$

$B_{sp}^p = \frac{2F_cM_{111}f_c}{W^p+w^s+w^p}$

$C_0^s = \frac{E_sE_p}{W^s+w^s+w^p}[f_c\frac{\kappa}{2}(a_1+2a_2-a_3)-f_s(w^sa_5+w^pa_4)]$

$C_s^s = (\frac{E_s^2}{W^s+2w^s}-\frac{f_c^2E_p^2}{W^s+2w^p})\frac{\kappa}{4}(-a_1+2a_2+a_3)$

$C_c^s = \frac{f_cE_sE_p}{W^s+w^s+w^p}\frac{\kappa}{2}(-a_1+2a_2+a_3)$

$C_0^p = -\frac{E_s^2}{W^p+2w^s}[F_sw^sa_7+F_c\frac{\kappa}{4}(a_1-2a_2+3a_3)]$
$-\frac{E_p^2}{W^p+2w^p}[F_sf_c^2w^pa_7-2F_sf_sf_c\kappa a_8+F_sf_s^2w^pa_9$
$+F_cf_c^2\frac{\kappa}{4}(3a_1+2a_2+a_3)-F_cf_sf_cw^p(a_4+a_5)+F_cf_s^2\kappa a_6]$

$C_s^p = \frac{F_cf_cE_sE_p}{W^p+w^s+w^p}\frac{\kappa}{2}(-a_1+2a_2+a_3)$

$C_c^p = (-\frac{F_cE_s^2}{W^p+2w^s}+\frac{F_cf_c^2E_p^2}{W^p+2w^p})\frac{\kappa}{4}(-a_1+2a_2+a_3)$

The integrations in Eqs. (36) and (37) can be evaluated explicitly and the final result for either *s*- or *p*-polarized SHG can be expressed as

$$E_{s,p}^{(2\omega)} = A_{s,p}(B_{ss}^{s,p}E_s^2 + B_{pp}^{s,p}E_p^2 + B_{sp}^{s,p}E_sE_p). \tag{39}$$

The SHG field can also be written in a form which emphasizes its dependence on the azimuthal angle ϕ,

$$E_{s,p}^{(2\omega)} = A_{s,p}(C_0^{s,p} + C_s^{s,p}\sin 4\phi + C_c^{s,p}\cos 4\phi). \tag{40}$$

The coefficients are listed in Table III.

Note that the fundamental fields E_s and E_p in the nonlinear medium are related to the incident field by Eq. (15). Therefore, to express the SHG field $E_{s,p}^{(2\omega)}$ in terms of the incident field, we can simply make the substitution $E_s = t_{01}^s E_{0s}$ and $E_p = t_{01}^p E_{0p}$ in Eqs. (39) and (40), where t_{01}^s and t_{01}^p have been written explicitly in Eq. (15).

IV. SURFACE CONTRIBUTION

Inversion symmetry is always broken at the surface of a crystal. As a result, second harmonic generation from electric dipole response exists within a few atomic layers of the surface. The source of second harmonic radiation in this region can be characterized by an effective surface polarization density, given in terms of a phenomenological surface nonlinear susceptibility tensor $\Delta^{(2)}$ by[2,9]

$$P_i^{s(2\omega)} = \sum_{j,k} \Delta_{ijk}^{(2)} E_j E_k \delta(z - 0^+). \tag{41}$$

The component of the microscopic electric field normal to the surface varies greatly over a few atomic layers near the surface, which itself contributes to the second harmonic generation. By convention the fields on the right hand side are evaluated inside the nonlinear medium and, as the delta function indicates, the polarization is placed just above the surface. Different conventions could be chosen, but they would only yield different phenomenological tensor components that could be related to the $\Delta_{ijk}^{(2)}$ in a trivial way.[28]

The calculations presented here are limited to surface contributions from the (001) crystal face. The calculations for other surface orientations can be done in a similar way by the methods outlined here. The allowed effective susceptibility tensor components $\Delta_{ijk}^{(2)}$ are determined by the symmetry of the surface region. For simplicity, we assume there is no surface reconstruction. Considering only the very top layer of the (001) face of tetragonal crystals, the appropriate symmetry is then C_{4v}, and in the crystal coordinate system the polarization takes the form[26]

$$\begin{bmatrix} P_x^{s(2\omega)} \\ P_y^{s(2\omega)} \\ P_z^{s(2\omega)} \end{bmatrix} = \begin{pmatrix} 0 & 0 & 0 & 0 & d_{15} & 0 \\ 0 & 0 & 0 & d_{15} & 0 & 0 \\ d_{31} & d_{31} & d_{33} & 0 & 0 & 0 \end{pmatrix} \begin{bmatrix} E_x^2 \\ E_y^2 \\ E_z^2 \\ 2E_yE_z \\ 2E_xE_z \\ 2E_xE_y \end{bmatrix}. \tag{42}$$

In dispersionless medium, one has $d_{15}=d_{31}$. Transforming the susceptibility from the crystal coordinates to the beam coordinates with the matrix V yields

$$\Delta'_{113} = \Delta'_{131} = \Delta'_{223} = \Delta'_{232} = d_{15},$$

$$\Delta'_{311} = \Delta'_{322} = d_{31}, \quad \Delta'_{333} = d_{33}, \tag{43}$$

where Δ'_{ijk} are the tensor elements of the surface in the beam coordinate system. Note that $\Delta'_{ijk}=\Delta_{ijk}$, i.e. the tensor for C_{4v} symmetry is unchanged under the rotation along $\hat{\mathbf{z}}$ direction. Therefore, the surface contribution will be independent of the azimuthal angle, ϕ, and in that sense isotropic. Following Sipe,[27] we write this polarization in the form

$$\mathbf{P}^{s(2\omega)}(\mathbf{r},t) = \mathbf{\Pi}^{(2\omega)} \delta(z - 0^+) e^{2i(\boldsymbol{\kappa}\cdot\mathbf{R} - \omega t)} + c.c., \tag{44}$$

with amplitude $\mathbf{\Pi}^{(2\omega)}$.

The total second harmonic wave generated from this surface polarization is obtained by adding the upward second harmonic wave with the downward harmonic wave reflected from the surface. Using the Green function method,[25,27] the SHG field at $z>0^+$ is given by

$$E_s^{(2\omega)} = \frac{i\tilde{\Omega}^2}{2\varepsilon_0 W_0}(1 + R_{01}^s)(\hat{\mathbf{s}} \cdot \mathbf{\Pi}), \tag{45}$$

$$E_p^{(2\omega)} = \frac{i\tilde{\Omega}^2}{2\varepsilon_0 W_0}(\hat{\mathbf{P}}_{0+} + R_{01}^p \hat{\mathbf{P}}_{0-}) \cdot \mathbf{\Pi}. \tag{46}$$

The Fresnel coefficients R_{01}^s, R_{01}^p, characterizing the reflection process of the downward going wave at the crystal surface are[25]

$$R_{01}^s = \frac{W_0 - W^s}{W_0 + W^s}, \quad R_{01}^p = \frac{W_0 \epsilon^{\parallel}(2\omega) - W^p}{W_0 \epsilon^{\parallel}(2\omega) + W^p}. \tag{47}$$

Finally, we obtain the SHG field generated from the surface polarization as

$$E_s^{(2\omega)} = \frac{i2\tilde{\Omega}^2}{\varepsilon_0(W_0 + W^s)} d_{15} f_s E_s E_p, \tag{48}$$

$$E_p^{(2\omega)} = \frac{i\tilde{\Omega}}{\varepsilon_0[W_0 \epsilon^{\parallel}(2\omega) + W^p]} \{K\epsilon^{\parallel}(2\omega) d_{31} E_s^2 + [K\epsilon^{\parallel}(2\omega)(d_{31} f_c^2 + d_{33} f_s^2) - 2W^p d_{15} f_c f_s] E_p^2\}. \tag{49}$$

We observe that the surface nonlinear susceptibility for tetragonal crystals with a (001) surface is identical to that of cubic crystals, because the surface symmetry is the same; differences in the surface SHG contributions only arise because of the different forms of the linear fields inside the two crystal classes. Therefore, two familiar results from the analysis of SHG at (001) surfaces of cubic crystals also hold here. First, the *s*-polarized SHG from surfaces only exists when the incident light has both *s*- and *p*-polarized components. Second, all the surface contributions are independent of the azimuthal angle ϕ.

V. ANALYSIS

The total SHG consists of both the bulk and the surface contributions. Therefore, it assumes a very complicated form. To extract useful information from the SHG, one needs to carefully design experimental configurations. Rotational-anisotropic SHG data can be acquired by rotating the sample to give a function that is ϕ dependent. Additionally, selecting the input and output polarization often reduces the number of tensor elements contributing to the SHG signal. Combinations of *s* or *p* input and output polarized rotational-anisotropic experiments provide a set of data that isolate the bulk and surface contributions. In the following, we suggest four experimental configurations.

Case 1. the incident light is *s*-polarized and the component of SHG that is analyzed has *s*-polarization. Only one term from the bulk contributes to the SHG,

$$E_s^{(2\omega)} = -\frac{i\tilde{\Omega}^2}{\varepsilon_0(W^s + W_0)} \frac{M_{111}}{W^s + 2w^s} (t_{01}^s)^2 E_{0s}^2. \tag{50}$$

Thus, the SHG intensity will be

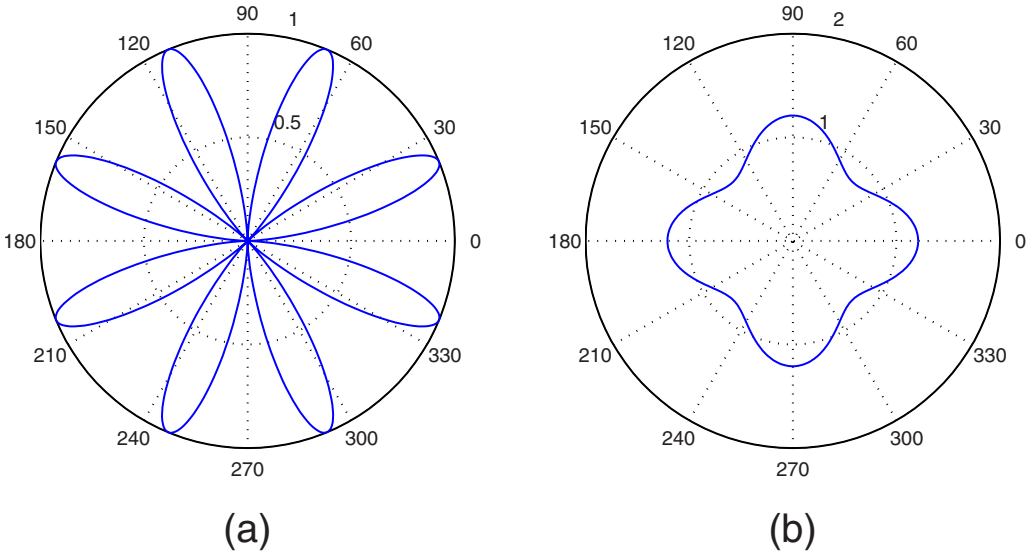

FIG. 2. (Color online) (a) Intensity for *s*-polarized SHG with s-polarized input as a function of angle ϕ. We normalize the prefactor of $\sin^2 4\phi$ to one in the plot. (b) Intensity for *p*-polarized SHG with *s*-polarized input as a function of angle ϕ. Since the surface response is usually much larger than the bulk response, we set $u=1$ and $v=0.1$ in Eq. (54).

$$I_{s\to s} = \frac{c}{32\varepsilon_0}\left|\frac{\kappa\tilde{\Omega}^2(t_{01}^s)^2E_{0s}^2(-a_1+2a_2+a_3)}{(W^s+W_0)(W^s+2w^s)}\right|^2 \sin^2 4\phi, \tag{51}$$

which exhibits an eight-fold symmetry with respect to angle ϕ and vanishes for $\phi=m\pi/4$, $m=0,1,\cdots,7$, as shown in Fig. 2(a). Using this configuration, we can measure the combined value of $(-a_1+2a_2+a_3)$.

Case 2. the incident light is *p*-polarized and the component of SHG that is analyzed has *s* polarization. This is similar to case 1, where only one bulk term contributes to the SHG. The field amplitude is

$$E_s^{(2\omega)} = \frac{i\tilde{\Omega}^2}{\varepsilon_0(W^s+W_0)}\frac{M_{111}}{W^s+2w^p}f_c^2(t_{01}^p)^2E_{0p}^2. \tag{52}$$

In this case, as with case 1, $I_{p\to s}\propto\sin^2 4\phi$, because they are both derived from tensor element M_{111}. Thus the factor of proportionality contains the term $(-a_1+2a_2+a_3)$. Compared with case 1, there is an extra factor f_c^2 in Eq. (52), which depends on the incident angle θ_0.

Case 3. the incident light is *s*-polarized and the component of SHG that is analyzed has *p*-polarization. In this case, we have both bulk and surface contributions. The field amplitude is

$$E_p^{(2\omega)} = \left[-\frac{i\tilde{\Omega}^2N}{\varepsilon_0[W^p+W_0\epsilon^{\parallel}(2\omega)]}\frac{F_sM_{311}-F_cM_{211}}{W^p+2w^s} + \frac{i\tilde{\Omega}K\epsilon^{\parallel}(2\omega)}{\varepsilon_0(W^p+W_0\epsilon^{\parallel}(2\omega))}d_{31}\right](t_{01}^s)^2E_{0s}^2. \tag{53}$$

Substituting M_{311} and M_{211} from Table II, the field amplitude takes the form $E_p^{(2\omega)}=u+v\cos 4\phi$ with some complex coefficients u and v. The surface term is independent of ϕ, hence it is contained in u. The intensity

$$I_{s\to p}\propto|E_p^{(2\omega)}|^2=|u|^2+|v|^2\cos^2 4\phi+2\,\mathrm{Re}(uv^*)\cos 4\phi, \tag{54}$$

will in general exhibit a four-fold symmetry with respect to angle ϕ. This behavior is shown in Fig. 2(b).

Case 4. the incident light is circularly polarized and the component of SHG that is analyzed has *s*-polarization. The quantity of interest in this case is the circular dichroism, which is defined as

$$D_c = \frac{I_{h_+\to s}-I_{h_-\to s}}{I_{h_+\to s}+I_{h_-\to s}}, \tag{55}$$

where $h_\pm$ denotes circularly polarized incident light with positive (negative) helicity, i.e., $E_{0s}=\pm iE_{0p}$. Circular dichroism in SHG is a powerful tool that has been widely used in studying the chiral properties of surfaces and biomolecules.[29] In addition, it has been proposed as a way to detect the hidden circulating current in the pseudogap phase of cuprates.[24] However, it has been demonstrated that nonlinear circular dichroism can also occur in surface films with in-plane anisotropy, even though the film is comprised of achiral chromophores.[30] In addition, SHG from oxidized Si (001) has been shown to exhibit a circular dichroism due to the interference between surface and bulk contributions.[31]

To calculate circular dichroism in SHG from tetragonal centrosymmetric crystals, without loss of generality one can write the total second harmonic field as

$$E_s^{(2\omega)} = gE_{0s}^2+hE_{0p}^2+lE_{0s}E_{0p}, \tag{56}$$

with complex coefficients g, h and l. For $h_\pm$ polarized light,

$$I_{h_\pm\to s} = |h-g\pm il|^2I_\omega^2, \tag{57}$$

where I_ω is the intensity of the incident light. Then the circular dichroism can be written as[31]

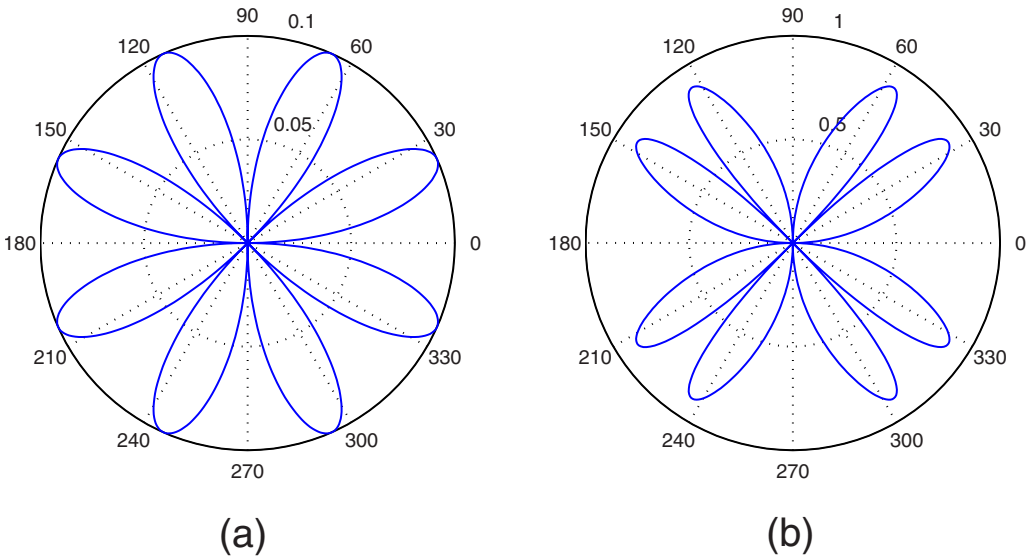

FIG. 3. (Color online) Circular dichroism of SHG as a function of angle ϕ plotted for two sets of parameters. (a) Assume the surface contribution is much larger than the bulk contribution. The parameters are set to $(H-G)=L_2=0.1i$, and $L_1=1+i$. The relative phase between $(H-G)$ and L_1 will only change the magnitude of D_c. (b) Assume the bulk contribution and the surface contribution are comparable. Set $(H-G)=L_2=i$ and $L_1=1+i$. A four-fold symmetry is clearly observed.

$$D_c = \frac{2\,\mathrm{Re}[(h-g)(il)^*]}{|h-g|^2+|il|^2}. \tag{58}$$

To observe circular dichroism, both $(h-g)$ and l must be nonzero and there must be a phase shift between them. To separate the azimuthal angle dependence of g, h, and l, we can write

$$g = G\sin 4\phi, \quad h = H\sin 4\phi, \quad l = L_1 + L_2\cos 4\phi, \tag{59}$$

where

$$G = -\frac{i\tilde{\Omega}^2\kappa(-a_1+2a_2+a_3)(t_{01}^s)^2}{4\varepsilon_0(W^s+W_0)(W^s+2w^s)}, \tag{60}$$

$$H = \frac{i\tilde{\Omega}^2\kappa(-a_1+2a_2+a_3)f_c^2(t_{01}^p)^2}{4\varepsilon_0(W^s+W_0)(W^s+2w^p)}, \tag{61}$$

$$L_1 = -\frac{i\tilde{\Omega}^2 t_{01}^s t_{01}^p\left[f_c\frac{\kappa}{2}(a_1+2a_2-a_3)-f_s(w^s a_5+w^p a_4)\right]}{\varepsilon_0(W^s+W_0)(W^s+w^s+w^p)} + \frac{2i\tilde{\Omega}^2}{\varepsilon_0(W^s+W_0)}d_{15}f_s t_{01}^s t_{01}^p, \tag{62}$$

$$L_2 = -\frac{i\tilde{\Omega}^2 f_c t_{01}^s t_{01}^p\frac{\kappa}{2}(-a_1+2a_2+a_3)}{\varepsilon_0(W^s+W_0)(W^s+w^s+w^p)}. \tag{63}$$

The surface contribution only enters into the coefficient L_1. Finally, the circular dichroism is expressed as

$$D_c = \frac{2\,\mathrm{Re}[(H-G)(iL_1)^*]\sin 4\phi + \mathrm{Re}[(H-G)(iL_2)^*]\sin 8\phi}{|H-G|^2\sin^2 4\phi + |L_1+L_2\cos 4\phi|^2}. \tag{64}$$

This expression has three complex terms, i.e., $(H-G)$, L_1, and L_2, which could be used as six fitting parameters to be determined experimentally. The dichroism should, in general, exhibit a four-fold symmetry with respect to the azimuthal angle and it vanishes at angles $\phi=m\pi/4$, $m=0,1,\cdots,7$. If we further assume the linear dielectric constants and the wave vectors of the light are real, then L_2 would be in phase with $(H-G)$. In that case, the expression for D_c is reduced to

$$D_c = \frac{2\,\mathrm{Re}[(H-G)(iL_1)^*]\sin 4\phi}{|H-G|^2\sin^2 4\phi + |L_1+L_2\cos 4\phi|^2}. \tag{65}$$

The angular dependence of D_c is shown in Fig. 3 for two conditions, where the surface contribution dominates or is comparable to the bulk terms.

A similar situation occurs for linear dichroism where the incident light polarization is chosen to be +45° vs. −45°. Then the s-polarized SHG intensity is

$$I_{\pm 45^\circ\to s} = |g-h\pm l|^2 I_\omega^2, \tag{66}$$

with linear dichroism,

$$D_l = \frac{I_{+45^\circ}-I_{-45^\circ}}{I_{+45^\circ}+I_{-45^\circ}} = \frac{2\,\mathrm{Re}[(g-h)l^*]}{|g-h|^2+|l|^2}. \tag{67}$$

In contrast to circular dichroism, the observation of linear dichroism does not require a phase shift between $(g-h)$ and l. By the substitution of (59), we obtain

$$D_l = \frac{2\,\mathrm{Re}[(G-H)L_1^*]\sin 4\phi + \mathrm{Re}[(G-H)L_2^*]\sin 8\phi}{|G-H|^2\sin^2 4\phi + |L_1 + L_2\cos 4\phi|^2}, \tag{68}$$

which also exhibits a four-fold symmetry in general.

SHG linear and circular dichroism exist in cubic crystals as well.[31] The result for tetragonal crystals discussed above recovers and agrees with that reported for cubic crystals if we impose further restrictions from cubic crystal symmetry. An important difference is that while dichroism in cubic crystals depends on just one surface element and one linear combination of bulk tensor elements $(a_1-2a_2-a_3)$ or $(\Gamma_{xxyy}+\Gamma_{xyxy}+\Gamma_{xyyx}-\Gamma_{xxxx})$, dichroism in tetragonal crystals depends on additional bulk elements.

VI. CONCLUSIONS

In conclusion, we have formulated a phenomenological theory of SHG from tetragonal centrosymmetric crystals. The theory is based entirely on symmetry considerations, and is thus generally applicable. We have suggested a few experimental configurations that can be used to extract information about particular nonlinear tensor elements and to analyze the symmetry of the SHG intensity pattern with respect to the azimuthal angle. We predict that there will be a nonzero dichroism in the SHG, which exhibits a four-fold symmetry.

ACKNOWLEDGMENTS

We are grateful to Junwei Wei, Alex Demkov, and Steve Cundiff for valuable discussions. We gratefully acknowledge financial support from the following sources: NSF under Grant No. DMR-0747822, ONR under Grant No. N00014-08-1-0745, Welch Foundation under Grant No. F-1662, Texas-ARP under Grant No. 003658-0160-2007, and the Alfred P. Sloan Foundation.

*Permanent address: Department of Physics and Institute for Optical Sciences, University of Toronto, 60 St. George Street, Toronto M5S 1A7, Canada.

[1] Y. R. Shen, *Principles of Nonlinear Optics* (Wiley, New York, 1984).
[2] H. W. K. Tom, T. F. Heinz, and Y. R. Shen, Phys. Rev. Lett. **51**, 1983 (1983).
[3] J. A. Litwin, J. E. Sipe, and H. M. van Driel, Phys. Rev. B **31**, 5543 (1985).
[4] P. Guyot-Sionnest, W. Chen, and Y. R. Shen, Phys. Rev. B **33**, 8254 (1986).
[5] See, for example, G. A. Reider and T. F. Heinz, in *Photonic Probes of Surfaces*, edited by P. Halevi (Elsevier, Amsterdam, 1995), pp. 413–478; P. F. Brevet, *Surface Second Harmonic Generation* (Presses Polytechniques et Universitaires Romandes, Lausanne, 1997); G. Lüpke, Surf. Sci. Rep. **35**, 75 (1999).
[6] P. S. Pershan, Phys. Rev. **130**, 919 (1963).
[7] N. Bloembergen and P. S. Pershan, Phys. Rev. **128**, 606 (1962); N. Bloembergen, R. K. Chang, S. S. Jha, and C. H. Lee, *ibid.* **174**, 813 (1968).
[8] C. C. Wang and W. W. Duminski, Phys. Rev. Lett. **20**, 668 (1968); C. C. Wang, Phys. Rev. **178**, 1457 (1969).
[9] J. E. Sipe, D. J. Moss, and H. M. van Driel, Phys. Rev. B **35**, 1129 (1987).
[10] G. A. Reider, U. Höfer, and T. F. Heinz, Phys. Rev. Lett. **66**, 1994 (1991); J. Chem. Phys. **94**, 4080 (1991); U. Höfer, L. Li, and T. F. Heinz, Phys. Rev. B **45**, 9485 (1992).
[11] W. Daum, H.-J. Krause, U. Reichel, and H. Ibach, Phys. Rev. Lett. **71**, 1234 (1993).
[12] G. Lüpke, D. J. Bottomley, and H. M. van Driel, Phys. Rev. B **47**, 10389 (1993).
[13] J. I. Dadap, B. Doris, Q. Deng, M. C. Downer, J. K. Lowell, and A. C. Diebold, Appl. Phys. Lett. **64**, 2139 (1994); J. I. Dadap, Z. Xu, X. F. Hu, M. C. Downer, N. M. Russell, J. G. Ekerdt, and O. A. Aktsipetrov, Phys. Rev. B **56**, 13367 (1997).
[14] S. T. Cundiff, W. H. Knox, F. H. Baumann, K. W. Evans-Lutterodt, M.-T. Tang, M. L. Green, and H. M. van Driel, Appl. Phys. Lett. **70**, 1414 (1997).
[15] Y. Q. An and S. T. Cundiff, Appl. Phys. Lett. **81**, 5174 (2002); Phys. Rev. B **67**, 193302 (2003); Y. Q. An, R. Carriles, and M. C. Downer, *ibid.* **75**, 241307(R) (2007).
[16] G. Lüpke, D. J. Bottomley, and H. M. van Driel, J. Opt. Soc. Am. B **11**, 33 (1994).
[17] J. F. McGilp, J. Phys.: Condens. Matter. **19**, 016006 (2007).
[18] X. Zhao, G. Yu, Y.-C. Cho, G. Chabot-Couture, N. Barisić, P. Bourges, N. Kaneko, Y. Li, L. Lu, E. M. Motoyama, O. P. Vajk, and M. Greven, Adv. Mater. **18**, 3243 (2006).
[19] J. Orenstein and A. J. Miller, Science **288**, 468 (2000).
[20] C. M. Varma, Phys. Rev. Lett. **83**, 3538 (1999).
[21] C. M. Varma, Phys. Rev. B **73**, 155113 (2006).
[22] A. Kaminski, S. Rosenkranz, H. M. Fretwell, J. C. Campuzano, Z. Li, H. Raffy, W. G. Cullen, H. You, C. G. Olson, C. M. Varma, and H. Hochst, Nature (London) **416**, 610 (2002).
[23] S. V. Borisenko, A. A. Kordyuk, A. Koitzsch, T. K. Kim, K. A. Nenkov, M. Knupfer, J. Fink, C. Grazioli, S. Turchini, and H. Berger, Phys. Rev. Lett. **92**, 207001 (2004).
[24] M. E. Simon and C. M. Varma, Phys. Rev. B **67**, 054511 (2003).
[25] J. J. Saarinen and J. E. Sipe, J. Mod. Opt. **55**, 13 (2008).
[26] R. W. Boyd, *Nonlinear Optics*, 2nd ed. (Academic Press, New York, 2002).
[27] J. E. Sipe, J. Opt. Soc. Am. B **4**, 481 (1987).
[28] T. F. Heinz, in *Nonlinear Surface Electromagnetic Phenomena*, edited by H.-E. Ponath and G. I. Stegeman (Elsevier, Amsterdam, 1991), p. 353.
[29] T. Petralli-Mallow, T. M. Wong, J. D. Byers, H. I. Yee, and J. M. Hicks, J. Phys. Chem. **97**, 1383 (1993).
[30] T. Verbiest, M. Kauranen, Y. VanRompaey, and A. Persoons, Phys. Rev. Lett. **77**, 1456 (1996).
[31] X. Li, J. Willits, S. T. Cundiff, I. M. P. Aarts, A. A E. Stevens, and D. S. Dessau, Appl. Phys. Lett. **89**, 022102 (2006).